Published in final edited form as:
J Labelled Comp Radiopharm. 2009 December 1; 52(14): 583–590. doi:10.1002/jlcr.1691.

^{111}In-labeled KCCYSL peptide as an imaging probe for ErbB-2-expressing ovarian carcinomas

Susan L. Deutscher[a,b], **Said D. Figueroa**[b], and **Senthil R. Kumar**[a,b,*]

[a]Department of Biochemistry, University of Missouri-Columbia School of Medicine, Columbia, MO 65211, USA

[b]Research Division, Harry S. Truman Veterans Hospital, Columbia MO 65201

Abstract

Aberrant expression of ErbB-2, a member of the epidermal growth factor family of receptors, has been implicated in the formation of various malignancies including ovarian cancer. The objective of this study was to determine if the bacteriophage (phage) display-selected ErbB-2 targeting peptide, KCCYSL, once radiolabeled with ^{111}In would serve as a tumor targeting and Single Photon Emission Computed Tomography (SPECT/CT) imaging agent in a mouse model of human ovarian carcinoma expressing ErbB-2. The KCCYSL peptide was synthesized with a chelator 1,4,7,10-tetra-azacyclododecane-N,N',N'',N'''-tetraacetic acid (DOTA), and a Gly-Ser-Gly (GSG) spacer between DOTA and amino terminus of the peptide and radiolabeled with $^{111}InC1_3$. In vitro cell binding studies indicated that ^{111}In-DOTA-GSG-KCCYSL bound to cultured ovcar-3 carcinoma cells. Biodistribution studies in scid mice bearing human ovcar-3 tumor xenografts revealed a tumor uptake of 0.50 ± 0.05 percent injected dose per gram (%ID/g) at 1 h, and 0.39 ± 0.1 %ID/g at 2 h. Blocking studies with non-radiolabeled counterpart indicated a partial inhibition (41%) ($P = 0.04$) in tumor uptake of ^{111}In-DOTA-GSG-KCCYSL. In vivo tumor uptake of ^{111}In-DOTA-GSG-KCCYSL was clearly evident through SPECT/CT images after 2 h post injection. These studies suggest the potential of this peptide as a radiopharmaceutical for imaging of ErbB-2-expressing ovarian tumors.

Keywords

Ovarian cancer; ErbB-2; peptide; radiolabeling; imaging

Introduction

Ovarian cancer is the second most common gynecologic malignancy in the United States, and has the highest mortality rate of all gynecologic cancers.1 Most patients with ovarian cancer are asymptomatic until the disease has metastasized. Roughly 70% of ovarian cancers are diagnosed at advanced stage and approximately 30% of women with such cancers can expect to survive 5 years.2 Hence, ovarian cancer poses a great challenge in gynecologic oncology. Identification of novel non-invasive tumor-targeting imaging probes could help to identify the ovarian tumor recurrence and could be translated into oncologic drugs or radiation therapeutic agents.

ErbB-2/Her2-neu is a receptor tyrosine kinase that is a member of EGFR family.3, 4 Notably, ErbB-2 acts as a ligand-less receptor that amplifies growth factor signaling.5 While

*Corresponding author: Senthil R. Kumar Department of Biochemistry 117 Schweitzer Hall University of Missouri Columbia, MO 65211 Tel: 573-814-6000 Ext: 53747 Fax: 573-882-5635.

low expression of ErbB-2 has been found in normal adult cells, amplification and consequent overexpression of ErbB-2 was observed in human breast, prostate, lung, gastric, and ovarian carcinomas.5,6 Several reports in the literature suggest varying percentage of ErbB-2 expression in ovarian tumor patients.7–11 Also, patients with ErbB-2-expressing ovarian carcinomas have a worse prognosis than those with ErbB-2-negative carcinomas.12 Association of ErbB-2 overexpression with poor prognosis of several types of carcinoma led to the recognition of the therapeutic potential of drugs that target this oncoprotein.5 Further, the elevated levels of ErbB-2 in many human malignancies and its extracellular presence make it an attractive target for the development of tumor specific ligands, which in turn may aid in the diagnosis of the disease.

Peptide and antibody ligands coupled to radionuclides have been applied in oncologic imaging of receptors and also have been successful in cancer therapy.13 Radiolabeled versions of somatostatin14 bombesin/gastrin releasing peptide,15 vasoactive intestinal peptide,16 and α-melanocyte stimulating hormone17 have been efficacious in cancer imaging and therapy. Strategies such as high-throughput screening and phage display are currently being employed to expand our repertoire of imaging probes. We previously identified peptides from phage display libraries that bound the recombinant extracellular domain of human ErbB-2.18 One of the isolated peptides, a hexameric peptide with the sequence KCCYSL, recognized recombinant ErbB-2 and human carcinoma cells overexpressing ErbB-2. This peptide, when radiolabeled with the gamma-emitting radionuclide ^{111}In, was able to successfully target and image ErbB-2 expressing human MDA-MB-435 breast tumor xenografts in mice.19 It is hypothesized that ^{111}In-DOTA-GSG-KCCYSL could function as an effective imaging agent for ErbB-2 expressing human ovarian carcinomas. The purpose of the current study was to evaluate whether ^{111}In-DOTA-GSG-KCCYSL peptide could bind *in vitro* human ovarian carcinoma cells (ovcar-3) that express ErbB-2 20 and *in vivo* image human ovarian tumors heterotransplanted in scid mice.

Experimental

Reagents and chemicals

Amino acids and resin were purchased from Advanced ChemTech (Louisville, KY). DOTA-tri-t-butylester was purchased from Macrocyclics, Inc (Richardson, TX). ^{111} In, in the form of $^{111}InCl_3$, was purchased from Mallinckrodt Chemicals (St. Louis, MO). All other reagents in this study were obtained from Fisher Scientific Company (Pittsburgh, PA) unless otherwise specified.

Cell lines

Human ovarian carcinoma cell line ovcar-3 was obtained from American Type Tissue Culture (ATCC). The normal human ovarian surface epithelial cell line HIO-80 was a kind gift from Dr. Andrew Godwin, Fox Chase Cancer Center (Philadelphia, PA). The ovcar-3 cells were maintained as monolayer cultures in RPMI-1640 medium supplemented with 20% FBS, sodium pyruvate, non-essential amino acids, and L-glutamine. The HIO-80 cells were maintained in a 1:1 mixture of medium 199 and MCDB-105 supplemented with 4% fetal bovine serum and 0.2 IU of pork insulin (Lilly, Indianapolis, IN) per ml. Cell cultures were maintained at 37°C in a 5% CO_2 humidified incubator.

Synthesis, radiolabeling, purification, and stability of ^{111}In-DOTA-GSG-peptide conjugates

The peptide KCCYSL, and its scrambled version, KYLCSC, were synthesized with a bifunctional chelator DOTA attached to the amino terminus of each peptide. Peptides were radiolabeled with ^{111}In and purified by reverse phase high-pressure liquid chromatography (RP-HPLC) essentially as described previously.19 Cell binding studies were performed with

both ^{111}In-DOTA-GSG-KCCYSL and ^{111}In-DOTA-GSG-KYLCSC. For pharmacokinetic studies, the purified ^{111}In-DOTA-GSG-KCCYSL was diluted with sterile saline to 0.185 MBq (5 μCi) per 100 μl. Imaging studies required concentration of RP-HPLC purified ^{111}In-DOTA-GSG-KCCYSL by Empore High Performance Extraction Disk cartridges (4215 HD) (Torrance, CA) and elution with distilled ethanol. Eluted ^{111}In-conjugated peptide was exposed under a stream of nitrogen to evaporate the ethanol, and diluted to the appropriate volume with sterile saline. In all cases, the concentration of ethanol in solution was below 4% before administration into the animal. All *in vitro* and *in vivo* analyses were carried out using the RP-HPLC-purified product. The stability of ^{111}In-DOTA-GSG-KCCYSL was determined as described earlier 19.

In vitro cell binding studies with radiolabeled peptide conjugates

The cell binding ability of ^{111}In-DOTA-GSG-KCCYSL or ^{111}In-DOTA-GSG-KYLCSC (negative control) (3×10^4 cpm) was evaluated with ErbB-2-expressing ovcar-3 cells and HIO-80 normal human ovarian epithelial cells (2.0×10^6 cells/tube), which express negligible levels of ErbB-2 essentially as mentioned previously 19.

The detection of ErbB-2 protein and α-tubulin in different cell lysates was performed by immunoblotting with anti-ErbB-2 (Stratagene (an Agilent Technologies Division), La Jolla, CA), and anti-α-tubulin antibodies (Cell Signaling Technology, Danvers, MA) respectively. The immunoreactive proteins were developed with peroxidase-conjugated anti-rabbit ErbB-2 and anti-rabbit α-tubulin antibodies and visualized by chemiluminescence detection system (Pierce).

In vitro competitive cell binding assay

The binding affinity of ^{111}In-DOTA-GSG-KCCYSL to ovcar-3 cells was examined by competitive displacement of non-radiolabeled DOTA-GSG-KCCYSL. In brief, 2.5×10^4 cpm of ^{111}In-DOTA-GSG-KCCYSL and increasing concentrations ($10^{-5} - 10^{-12}$ M) of DOTA-GSG-KCCYSL were incubated for 45 min at 37°C with ovcar-3 cells (2.5×10^6 cells/tube) in cell binding media. At the end of the incubation period, the medium was aspirated after pelleting the cells by centrifugation. The cell pellet was further washed three times with 0.5 ml of ice-cold binding buffer to remove any unbound radioactivity. The remaining cell-bound radioactivity was counted using a γ counter. The ligand concentrations that inhibited 50% of the maximum specific binding (IC_{50}) were determined using Grafit software (Erithacus Software Limited, Surrey, UK).

In vitro internalization studies

The degree of peptide internalization in ovcar-3 cells (2.5×10^6/tube) was tested by incubating ~ 2.5×10^4 cpm ^{111}In-DOTA-GSG-KCCYSL at 37°C in the presence of 5% CO_2 at 10-, 20-, 40-, 60-, 90- and 120 min time points (n=3) as mentioned earlier 19.

Pharmacokinetic studies in ovcar-3 xenografted scid mice

Animal studies were conducted in compliance with Institutional Animal Care and Use Committee approval. Female 4–6 week old scid (ICR scid) mice were obtained from Taconic (Hudson, NY). Approximately, 1×10^7 ovcar-3 human ovarian carcinoma cells were implanted subcutaneously in the right shoulder of each scid mouse under gas anesthesia (3.5% isoflurane, Baxter Healthcare Corp. Deerfield, IL) and ~ 1L/min oxygen. Each mouse received a tail vein bolus of 0.185 MBq (5 μCi) of the radio-RP-HPLC peak purified ^{111}In-DOTA-GSG-KCCYSL in 100 μl saline. The mice were sacrificed by cervical dislocation and their tissues and organs excised at 1, 2, 4, and 24 h time points post injection (p.i). Three mice per time point were used. The excised tissues were weighed, and the tissue

radioactivity was measured in a γ counter, and the %ID or %ID/g were determined for each tissue. Whole blood %ID and %ID/g were determined under the assumption that the weight of the blood accounted for 6.5% of the body weight of the mouse.

The tumor uptake specificity of ^{111}In-DOTA-GSG-KCCYSL was determined by blocking tumor uptake at 2 h p.i. with the administration of 100 μg of non-radiolabeled In-DOTA-GSG-KCCYSL, 20 min before injecting 0.185 MBq (5 μCi) of the radiolabeled peptide. An amino acid lysine co-infusion experiment was performed in scid mice to observe the blocking effect of the amino acid on the kidney uptake of ^{111}In-DOTA-GSG-KCCYSL. One set of scid mice (n=3) received a tail vein injection of 0.185 MBq (5 μCi) ^{111}In-DOTA-GSG-KCCYSL along with 100 μg of lysine, while the other set of animals received the radiolabeled peptide (0.185 MBq, 5 μCi) only. The biodistribution study was performed after 2 h p.i. to assess the difference in the uptake of radioactivity in the kidneys.

MicroSPECT/microCT studies

Imaging was performed on human ovcar-3 tumor xenografted scid mice after 2 h p.i. of ^{111}In-DOTA-GSG-KCCYSL in a MicroSPECT (microCAT II, Siemens Pre-Clinical Solutions, Knoxville, TN) equipped with dual pixilated SPECT detectors each coupled to a square 3 × 3 array of position sensitive photomultiplier tubes. The ovcar-3 tumor xenografted scid mice were administered up to 11.1 MBq (300 μCi) of ^{111}In-DOTA-GSG-KCCYSL via tail vein injection. For imaging, mice were euthanized at the end of 2 h by CO_2 inhalation. MicroSPECT scans of 60 frames were acquired for a total count acquisition of 0.5 million counts for ^{111}In-DOTA-GSG-KCCYSL. A pinhole magnification factor of 2.2 was used in the experiments. The SPECT projection data were reconstructed using a 3D-OSEM algorithm. MicroCT (Siemens Pre-Clinical Solutions, Knoxville, TN) imaging was performed for 8 min and the data were reconstructed through a cone beam (Feldkamp) filtered backprojection algorithm. The data reconstructed from SPECT and CT was visualized and co-registered using Amira 3.1 software (TGS, San Diego, CA).

Statistical analysis

Data are expressed as mean ± SD. Mean values were compared using the Student's t test. Significance comparisons were made for blocking experiments during in vivo biodistribution studies. Differences were considered statistically significant for $P \leq 0.05$

Results and discussion

The KCCYSL peptide was synthesized with the bifuntional chelator DOTA conjugated to the amino terminus of the peptide via a GSG spacer between the peptide and DOTA to avoid any possible steric hindrance. The synthesized DOTA-GSG-KCCYSL peptide was labeled with ^{111}In using a 0.1 M NH_4OAc solution at pH 5.5 (Figure 1), and was separated from its non-labeled counterpart by RP-HPLC. Radiolabeling efficiency was ~ 40–45%. The radiochemical purity of the peptide was more than 97%, and the yield after purification was 35% with a specific activity of 65.4 GBq/μmol. The scrambled version of the peptide, DOTA-GSG-KYLCSC was similarly radiolabeled and purified. Radiochemical stability of the ^{111}In-DOTA-GSG-KCCYSL peptide was assayed in 0.01M PBS/0.1%BSA, pH 7.4 at 37°C. Over 24 h incubation period, only radiolabeled peptide, not free radioactivity, was detected by RP-HPLC (data not shown).

The *in vitro* receptor binding properties of the purified peptides, ^{111}In-DOTA-GSG-KCCYSL and ^{111}In-DOTA-GSG-KYLCSC, was tested with cultured human ovcar-3 cells (previously isolated from the ascites of a patient with progressive adenocarcinoma of the ovary20 expressing ErbB-2). A similar study was performed with normal ovarian epithelial (HIO-80) cells that express negligible levels of ErbB-2, which served as a negative control.

The expression patterns of ErbB-2 protein in these cell lines were determined by immunoblotting experiments (Figure 2A). The time course of cell binding shown in Figure 2B, indicate that ^{111}In-DOTA-GSG-KCCYSL association to ovcar-3 cells increased gradually and equilibrium was reached at 90 min, beyond which no further increase in cell-associated radioactivity was observed. This result indicated that binding of ^{111}In-DOTA-GSG-KCCYSL to cultured ovcar-3 cells was specific. On the other hand, negligible binding of the peptide to HIO-80 control cells was observed. Unlike ^{111}In-DOTA-GSG-KCCYSL, studies with the radiolabeled scrambled ^{111}DOTA-GSG-KYLCSC peptide indicated that binding to both HIO-80 and ovcar-3 cells was very low (Figure 2B).

In vitro competitive binding studies with ^{111}In-DOTA-GSG-KCCYSL were performed using cultured ovcar-3 cells. The competitive binding curve for the radiolabeled peptide with competition against various concentrations of non-radioactive DOTA-GSG-KCCYSL is shown in Figure 3. Radioactivity bound to cultured ovcar-3 carcinoma cells decreased with addition of increasing concentration ($10^{-12} - 10^{-5}$ M) of its non-radiolabeled counterpart. Analysis of the binding data indicated that ^{111}In-DOTA-GSG-KCCYSL demonstrated nanomolar affinity (47 ± 10.2 nM) for ovcar-3 cells expressing ErbB-2. This was comparable to the IC_{50} values of 42.5 ± 2.76 nM of ^{111}In-DOTA-GSG-KCCYSL peptide previously obtained with MDA-MB-435 human breast carcinoma cells .19

Cell internalization is the process of accumulation of radioconjugates over time within cells expressing the targeted receptors. The internalization ability of ^{111}In-DOTA-GSG-KCCYSL was analyzed in ovcar-3 cells. Results indicated that the majority of the peptide-associated radioactivity was on the cell surface with negligible internalization (~ 3%) inside the cells (Figure 4. However, in our earlier studies, a minimal but increased internalization of the ^{111}In-DOTA-GSG-KCCYSL by MDA-MB-435 human breast carcinoma cells (~ 11%), was observed. It is known that cultured cancer cell lines often differ in their cellular processing of the same receptor due to genetic instabilities.21 In this context, recent studies with the anti-ErbB-2 synthetic affibody monomer, ^{111}In-DOTA-Z_{HER2}:342-pep2 indicated that radioactivity was primarily membrane bound and the internalized fraction was relatively small (20%) in ErbB-2 expressing breast (SKBR-3) and ovarian carcinoma cells (SKOV-3). 21 Cell type-dependant endocytic internalization was also reported for an artificial ErbB-2 binding ligand.22 Further, depending on the nature of the radiolabel, degradation products either diffuse from cells or become trapped intracellularly.23 Moreover, in contrast to EGFR, ErbB-2 is known to remain at the plasma membrane after ligand binding24 and remains as an internalization-resistant receptor.25 Therefore, the degree of internalization of ErbB-2 receptors may vary between different carcinoma cells.

Radioactive compound stability is critical in that the molecular integrity of the radiopharmaceutical should be maintained for adequate times in the blood circulation during biodistribution and imaging studies. ^{111}In-DOTA-GSG-KCCYSL was inherently stable in phosphate buffer (pH 7.4) for a prolonged period of 24 h. Also, we reported in our previous study 26 that the peptide was stable in mouse serum for a period of 2 h, after which slow degradation was observed. Proteolytic degradation can occur in the serum or during transit of the peptide through the liver, kidneys or the gastrointestinal tract which might contribute to the instability of the radiotracer.26 Previous studies demonstrated that a 12-amino acid synthetic peptide radiolabeled with iodine, ^{125}I-FROP-1 (EDYELMDLLAYL), selected by phage display for targeting thyroid carcinoma cells was found to be unstable and degraded within 30 min of incubation in serum.27

The *in vivo* pharmacokinetics of ^{111}In-DOTA-GSG-KCCYSL were examined in scid mice bearing ovcar-3 tumor xenografts at 1, 2, 4 and 24 h p.i., and the results are summarized in Table 1. The tumor uptake of the radiotracer was 0.5 ± 0.05 %ID/g, 0.39 ± 0.10 %ID/g, 0.15

± 0.01%ID/g and 0.09 ± 0.03 %ID/g at 1, 2, 4 and 24 h, respectively. The radioconjugates cleared from the blood efficiently with 0.23 ± 0.07 %ID/g at 1 h followed by rapid decline at 2 h (0.13 ± 0.03 %ID/g) and 4 h (0.07 ± 0.00 %ID/g). At 2 h p.i., the tumor retention of the radioactivity was 3 fold higher than that present in the blood suggesting that the tumor radioactivity was not merely due to permeabilization of the tissue by circulating blood, but rather retention of the radioconjugate in the tumor tissue. Moderate uptake of radioactivity (0.34 ± 0.02 %ID/g) was observed in the lungs at 1 h which gradually declined to 0.12 ± 0.03 at 4 h. Minimal uptake was also observed in non-target tissues such as liver and gastrointestinal tract. Out of all non-target-tissues, the kidneys retained appreciable radioactivity with 3.01 ± 0.73 %ID/g at 2 h, followed by a decline to 1.35 ± 0.23 %ID/g at 24 h. Clearance of the radioconjugate from the mice appeared to occur primarily through the renal/urinary system. Approximately 95.6 ± 1.06 %ID of the radioconjugate was excreted from the mouse at the end of 1 h, while the excretion through the hepatobiliary system for the same time point was 0.17 ± 0.03 %ID (data not shown). Increased tumor-to-muscle (13.0) and tumor-to-blood (3.0) ratios at the end of 2 h using a radiolocalization index (%ID/g of tumor / %ID/g of nontarget tissue) are shown in Table 1.

Our studies with ^{111}In-DOTA-GSG-KCCYSL indicated that circulation in blood dropped rapidly within 4 h to 0.07 ± 0.0 ID/g. Also, as anticipated, the clearance of the peptide from the whole body occurred through the urinary tract. Such clearance contributed to reasonable tumor-to-nontarget ratios in ovcar-3 xenografed mice. Low background radioactivity levels could also be partly attributed to the stability of the DOTA chelating moiety. On the otherhand, an unstable peptide-radiometal complex could result in free ^{111}In in the circulation which could be retained by metal-binding proteins and eventually clear slowly from the circulation, thus contributing to high background radioactivity. Biodistribution studies also indicated lung uptake of the ^{111}In-DOTA-GSG-KCCYSL peptide. However, in the present study it is not clear whether ovcar-3 cells metastasized to the lungs and the radiolabeled peptide was binding specifically here. Previous studies indicated that NIH-ovcar-3 cells injected into athymic nude mice produce two morphologically distinct tumor cell populations (ascites and solid tumors), and the ascites tumor cells with increased motility may contribute to metastasis.28 Another study reported that lung metastatic tumors were usually detected in the high metastatic cell line ovcar-3.29

In order to determine the tumor uptake specificity of the radioconjugate *in vivo*, blocking studies were performed with 100 μg of non-radioactive DOTA-GSG-KCCYSL which was administered in ovcar-3 tumor mice (n=3) 15 min before injection of its ^{111}Inradiolabeled counterpart. Injection of the cold peptide reduced approximately 59% of the radiolabeled peptide uptake in tumor tissue (Table 1) compared to mice injected with radioactive peptide alone ($P = 0.04$).

The kidney retention of ^{111}In-DOTA-GSG-KCCYSL was high. For ovarian cancer radioimaging, it would be prudent to minimize the background noise in the abdominal organs, more specifically the kidneys. The infusion of basic amino acids such as L-lysine or L-arginine for inhibition of renal uptake of the radiolabeled peptides has been well documented.30–32 Therefore, we performed blocking experiments with the amino acid lysine, to hinder the kidney uptake of the radiolabeled peptide (Figure 5). The results indicated a partial inhibition (~ 30%) of kidney radioligand uptake in lysine co-infused animals compared to the radiolabeled peptide only group. No significant difference in the uptake of the radiolabeled peptide with lysine infusion in other tissues was observed. Lysine block was a useful approach, but was not effective enough to significantly reduce non-specific retention. Alternate options for reducing nonspecific kidney uptake of the radiolabeled peptide might include the use of gelatin based plasma expanders33 or low molecular weight peptide fragments from albumin.34

The axial, volume rendered CT, and fused microSPECT/CT whole body images of ovcar-3 tumor-bearing scid mice are shown in Figure 6. Following administration of 11.1 MBq (300 μCi) of ^{111}In-DOTA-GSG-KCCYSL, the images were acquired 2 h later in order to achieve good tumor to background signal. Inspection of the whole body image illustrated good tumor visualization with this radiotracer, and correlated well with the pharmacokinetic studies at 2 h p.i. Further, the axial image demonstrated reasonable accumulation of radioactivity in the tumor tissue. Though the radioactive accumulation in collateral tissues was minimal, substantial radioactivity accumulated in the kidneys, and was clearly evident in the SPECT/CT image, which is in keeping with the *in vivo* biodistribution studies (Table 1). Because of reasonable tumor retention and biologic clearance of the radiolabeled peptide, there was significantly less background activity observed with the SPECT image. While the imaging studies indicated the specific tumor binding property of ^{111}In-DOTA-GSG-KCCYSL, the kidney uptake of this peptide could be due to non-specific accumulation in this organ. Uptake of radiolabeled peptide in non-target tissues such as liver and kidneys have been reported in previous studies with a colon cancer targeting ^{111}In-labeled DOTA cyclic peptide (DOTA-RPMC) derived from phage display.35 Another study with a ^{99}Tc-labeled bombesin-like peptide, demonstrated good tumor uptake and relatively faster blood clearance but significant uptake in the liver, intestine and kidneys in a small cell lung cancer transplanted mice.36

Previous studies with positron emission tomography (PET) using F-18-fluorodeoxyglucose (FDG) in patients has been shown to identify primary tumors, and distant metastases for various tumor types including primary and recurrent ovarian cancer.37,38 However, variable radioactivity is seen in stomach and bowel, and a faint uptake was seen in liver and spleen. 39.40 There is also excretion of FDG by the kidneys, which led to renal, urethral and bladder activity. All these could lower the specificity of PET imaging with FDG. In contrast, our preliminary studies in mice indicated specific uptake of radiotracer by the ovarian tumor as visualized by SPECT/CT, and very minimal uptake in non-target tissues except for kidneys. While this could improve the specificity of imaging, the role of different imaging modalities in the assessment of various ovarian cancer conditions, such as characterization of ovarian mass, assessing extrapelvic spread of disease as well as detection of recurrent disease could vary. Additionally, the specificity of imaging of ovarian tumors in its anatomic location could also be compromised by the normal bladder and bowel physiologic activity40 in the abdomen. Hence, a combined multimodality imaging such as PET/CT or SPECT/CT along with ultrasound, and magnetic resonance would be beneficial for functional and anatomic imaging in ovarian carcinoma. Since our study was performed in a shoulder xenograft mouse model, it may not exactly mirror the studies performed in human subjects37,38 with ovarian tumors. Nevertheless, our studies indicate a combinatorial peptide based receptor targeting approach for SPECT/CT imaging of ErbB-2 positive ovarian tumors, which may be developed for clinical applications presumably for recurrent ovarian tumors.

Conclusions

We evaluated ^{111}In-DOTA-GSG-KCCYSL as a potential SPECT tracer for imaging human ovarian tumor in mice. The peptide clearance from the blood and excretion were rapid. Biodistribution and imaging studies indicated tumor uptake of the peptide. Lysine block partially inhibited the kidney uptake of the radiolabeled peptide. Additional studies are required to address the possibility of further minimizing radiolabel retention in the kidney. Overall, our results have demonstrated that ^{111}In-DOTA-GSG-KCCYSL may act as valuable diagnostic probe for certain ErbB-2 expressing ovarian carcinomas.

Supplementary Material

Refer to Web version on PubMed Central for supplementary material.

Acknowledgments

This work was supported by awards from the National Institutes of Health, (P50CA103130-01, 1R-21CA137239-01A1) and in part by a Merit Review Award from the Veterans Administration to SLD. We thank the VA Biomolecular Imaging Center at the Harry S. Truman Memorial Veterans' Hospital and the University of Missouri-Columbia for their support. We also thank Dr. Thomas Quinn for helpful suggestions, Lisa Watkinson and Terry Carmack for performing animal experiments and Marie Dickerson for technical help.

References

[1]. Jemal A, Siegel R, Ward E, Hao Y, Xu J, Murray T, Thun MJ. CA Cancer. J. Clin. 2008; 58:71–96. [PubMed: 18287387]

[2]. Cho KR, Shih I-M. Ann. Rev. Pathol. Mech. Dis. 2000; 4:287–313.

[3]. Bargmann CL, HungM-C M-C, Weinberg RA. Nature. 1986; 319:226–230. [PubMed: 3945311]

[4]. Yamamoto T, Ikawa S, Akiyama T, Semba K, Nomura N, Miyajima N, Saito T, Toyoshima K. Nature. 1986; 319:230–234. [PubMed: 3003577]

[5]. Citri A, Alroy I, Lavi S, Rubin C, Xu W, Grammatikaki N, Patterson C, Neckers L, Fry DW, Yarden Y. EMBO. J. 2002; 21:2407–2417. [PubMed: 12006493]

[6]. Klapper LN, Waterman H, Sela M, Yarden Y. Cancer. Res. 2000; 60:3383–88.

[7]. Felip E, Del Campo JM, Rubio D, Vidal MT, Colomer R, Bermejo B. Cancer. 1995; 75:2147–52. [PubMed: 7697606]

[8]. Hung M, Zhang X, Yan DH, Zhang HZ, He G, Zhang TQ, Shi DR. Cancer. Lett. 1992; 61:95–103. [PubMed: 1346099]

[9]. Kacinsky BM, Mayer AG, King BL, Carter D, Chambers SK. Gynecol. Oncol. 1992; 44:245–53. [PubMed: 1347282]

[10]. Haldane JS, Hird V, Hughes CM, Gullick WJ. J. Pathol. 1990; 162:231–7. [PubMed: 2266460]

[11]. Rubin SC, Finstad CL, Wong GY, Alamdrones L, Plante M, Lloyd KO. Am. J. Obstet. Gynecol. 1993; 168:162–9. [PubMed: 8093588]

[12]. Vernimmen D, Gueders M, Pisvin S, Delvenne P, Winkler R. Br. J. Cancer. 2003; 89:899–906. [PubMed: 12942124]

[13]. Kelloff GJ, Krohn KA, Larson SM, Weissleder R, Mankoff DA, Hoffman JM, Link JM, Guyton KZ, Eckelman WC, Scher HI, O'Shaughnessy J, Cheson BD, Sigman CC, Tatum JL, Mills GQ, Sullivan DC, Woodcock J. Clin. Cancer. Res. 2005; 11:7967–85. [PubMed: 16299226]

[14]. Bakker WH, Krenning EP, Reubi JC, Breeman WA, Setyono-Han B, de Jong M. Life. Sci. 1991; 49:1593–1601. [PubMed: 1658516]

[15]. Van de Wiele C, Dumont F, Dierckx RA, Peers SH, Thornback JR, Slegers G, Thierens H. J. Nucl. Med. 2001; 42:1722–27. [PubMed: 11696645]

[16]. Virgolini I. European. J. Clin. Invest. 1997; 27:793–800.

[17]. Chen J J, Cheng Z, Hoffman TJ, Jurisson SS, Quinn TP. Cancer. Res. 2000; 60:5649–58. [PubMed: 11059756]

[18]. Karasseva NG, Glinsky VV, Chen NX, Komatireddy R, Quinn TP. J. Protein. Chem. 2002; 21:287–96. [PubMed: 12168699]

[19]. Kumar SR, Quinn TP, Deutscher SL. Clin. Cancer. Res. 2007; 13:6070–79. [PubMed: 17947470]

[20]. Hamilton TC, Young RC, McKoy WM, Grotzinger KR, Green JA, Chu EW, Whang-Peng J, Rogan AM, Green WR, Ozols RF. Cancer.Res. 1983; 43:5379–89. [PubMed: 6604576]

[21]. Wållberg H, Orlova A. Cancer. Biotherm. Radiopharm. 2008; 23:435–42.

[22]. Hashizume T, Fukuda T, Nagaoka T, Tad H, Yamada H, Watanabe K, Salomon DS, Seno M. Cell. Biol. Int. 2008; 32:814–826. [PubMed: 18442934]

[23]. James JL, Moyer BR, Dean RT, Dean Q. J. Nucl. Med. 1997; 41:111–118.

[24]. Yarden Y. Oncology. 2001; 61:1–13. [PubMed: 11694782]

[25]. Hommelgaard AM, Lerdrup M, van Deurs B. Mol. Biol. Cell. 2004; 15:1557–67. [PubMed: 14742716]

[26]. Jain RK. J. Control. Release. 1998; 53:49–67. [PubMed: 9741913]

[27]. Zitzmann S, Krämer S, Mier W, Hebling U, Altmann A, Rother A, Berndorff D, Eisenhut M, Haberkorn U. J Nucl Med. 2007; 48:965–72. [PubMed: 17504878]

[28]. Veatch AL, Carson LF, Ramakrishnan S. Clin Exp Metastasis. 1995; 13:165–72. [PubMed: 7750204]

[29]. Qinglei G, Ding M, Li M, Shixuan W, Chanyu W, Yungpin L, Ali Z, Zing L. The Chinese-German J of Clin Oncol. 2004; 3:97–100.

[30]. Behr TM, Sharkey RM RM, Juweid ME, Blumenthal RD, Dunn RM, Griffiths GL, Bair HJ, Wolf FG, Becker WS, Goldenber DM. Cancer. Res. 1995; 55:3825–34. [PubMed: 7641200]

[31]. Behr TM, Becker WS, Sharkey RM, Juweid ME, Dunn RM, Bair HJ, Wolf FG, Goldenberg DM. J. Nucl. Med. 1996; 37:829–33. [PubMed: 8965154]

[32]. Behr TM, Goldenberg DM, Becker W. Eur. J. Nucl. Med. 1998; 25:201–12. [PubMed: 9473271]

[33]. Vegt E, Wetzels JF, Russel FG, Masereeuw R, Boerman OC, van Eerd JE. J. Nucl. Med. 2006; 47:432–36. [PubMed: 16513612]

[34]. Vegt E, van Eerd JE, Eek A, Oyen WJ, Wetzels JF, de Jong M, Russel FG, Masereeuw R, Gotthardt M, Boerman OC. J. Nucl. Med. 2008; 49:1506–11. [PubMed: 18703613]

[35]. Kelly K, Alencar H, Funovics M, Mahmood U, Weissleder R. Cancer Res. 2004; 64:6247–51. [PubMed: 15342411]

[36]. Varvarigou AD, Scopinaro F, Leondiadis L, Corleto V, Schillaci O, De Vincentis G, Sourlingas TG, Sekeri-Pataryas KE, Evangelatos GP, Leonti A, Xanthopoulos S, Delle Fave G, Archimandritis SC. Cancer Biother Radiopharm. 2002; 17:317–26. [PubMed: 12136524]

[37]. Fenchel S, Grab D, Nuessle K, Kotzerke J, Rieber A, Kreienberg R, Brambs HJ, Reske SN. Radiology. 2002; 22:780–8. [PubMed: 12034950]

[38]. Rohren EM, Turkington TG, Coleman RE. Radiology. 2004; 231:305–32. [PubMed: 15044750]

[39]. Wahl, RL.; Buchnan, JW. Principles and practice of positron emission tomography. Lippincot Williams & Wilkins; Philadelphia: 2002.

[40]. Rose PG, Faulhaber P, Miraldi F, Abdul-Karim FW. Gynecol. Oncol. 2001; 82:17–21. [PubMed: 11426956]

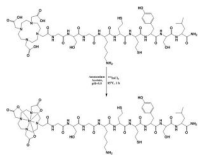

Figure 1.
Scheme for ^{111}In radiolabeling of DOTA-GSG-KCCYSL.

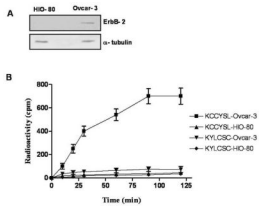

Figure 2.

Western blot showing the relative expression of (**A**) ErbB-2 (~ 185 kDa) in ovcar-3 and HIO-80 total cell lysates (40 μg each). Cytoplasmic marker α-tubulin (~ 50 kDa) was used to determine equal loading of proteins. (B) for determining the cell binding properties of ^{111}In-labeled peptides, approximately 2.0 ×10^6 cells per tube were incubated at 37°C for different time intervals with 3.0 ×10^4cpm ^{111}In-DOTA-GSG-KCCYSL or scrambled ^{111}In-DOTA-GSG-KYLCSC (n=3 each time point). While ^{111}In-DOTA-GSG-KCCYSL binding to human ovcar-3 carcinoma cells was observed, only minimal binding was seen with normal ovarian epithelial HIO-80 cells that express very little ErbB-2. ^{111}In-DOTA-GSG-KYLCSC did not show significant binding to either ovcar-3 or HIO-80 cell lines.

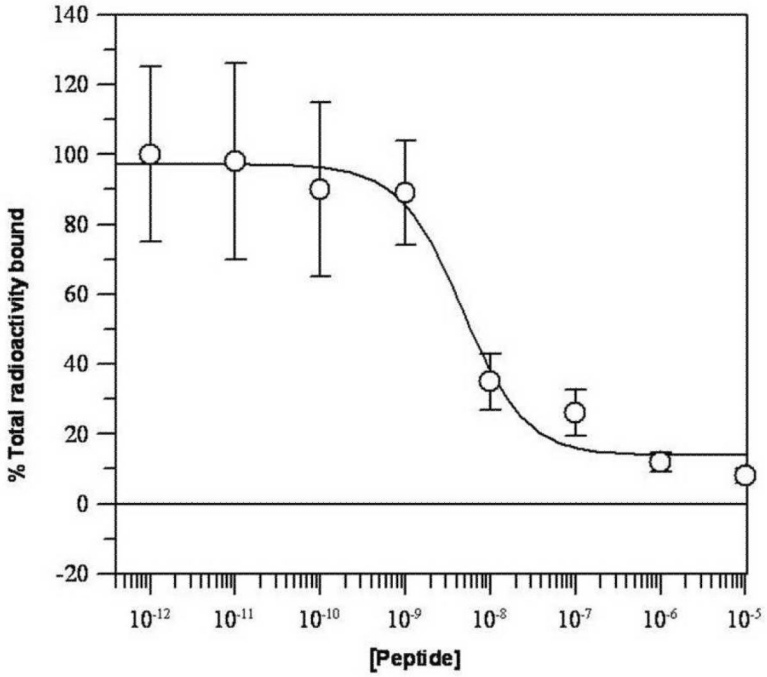

Figure 3.

Competitive binding assay of DOTA-GSG-KCCYSL against ^{111}In-DOTA-GSG-KCCYSL. Ovcar-3 cells (2.5×10^6 cells/tube) were incubated with radioligand (2.5×10^4 cpm) and increasing concentrations of non-radioactive peptide ($10^{-12} - 10^{-5}$ M) (n=3). The cell-bound radioactivity was counted using a Wallac γ counter. A binding affinity with the 50% inhibitory concentration (IC_{50}) of 47 ± 10.2 nM was obtained as determined by the Grafit software program.

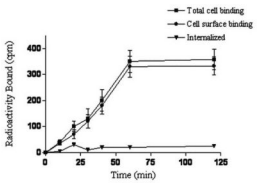

Figure 4.

Cell internalization of ^{111}In-DOTA-GSG-KCCYSL. Peptide internalization studies were performed by incubating ovcar-3 cells (2.5×10^6 cells/tube) along with ~ 2.5×10^4 cpm ^{111}In-DOTA-GSG-KCCYSL at 37°C in the presence of 5% CO_2 at different time points (n=3). The radioactivity was measured in the supernatant and the cells as a function of time.

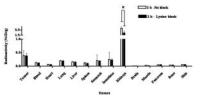

Figure 5.

Effect of lysine on the kidney uptake of ^{111}In-DOTA-GSG-KCCYSL. Ovcar-3 xenografted scid mice (n = 3 each) were injected with 0.185 MBq (5 μCi) of radiolabeled peptide only or co-injected with radiolabeled peptide and lysine (100 μg). The animals were sacrificed 2 h after injection, and the radioactivity associated with tissues including the kidneys was measured using a Wallac γ counter. Data are expressed as %ID/g (mean with SD). $P \leq 0.04$, significance comparison between the kidney uptake of radiolabeled peptide in the presence or absence of amino acid lysine at 2 h post injection.

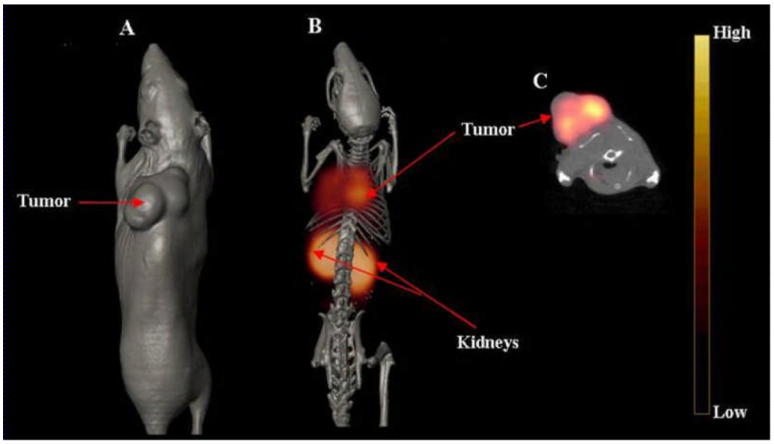

Figure 6.

In vivo microSPECT/CT of ovcar-3 tumor-bearing mice. ^{111}In-DOTA-GSG-KCCYSL 11.1 MBq (300 μCi) was injected in the tail vein of a scid mouse bearing a human ovcar-3 tumor xenograft. Imaging was acquired 2 h after injection. (**A**) Volume rendered CT image; (**B**) co-registered micro SPECT/CT image, (microSPECT images were fused with anatomical data from microCT images to validate regions of increased radiolabeled ligand uptake); and (**C**) microSPECT/CT axial image, view focusing on tumor uptake of the radiolabeled peptide. Imaging was performed in a MicroCAT IITM CT/SPECT (Siemens Pre-Clinical Solutions, Knoxville, TN) scanner equipped with a high resolution 2-mm pinhole collimator.

J Labelled Comp Radiopharm. Author manuscript; available in PMC 2010 December 1.

Table 1

Pharmacokinetics of ^{111}In-DOTA-GSG-KCCYSL in ovcar-3 tumor bearing scid mice at different time intervals (n =3).

Tissues	1 h	2 h	2 h block	4 h	24 h
Percent injected dose/gram (%ID/g)					
Tumor	0.50 ± 0.05	0.39 ± 0.10	0.16 ± 0.03*	0.15 ± 0.01	0.09 ± 0.03
Blood	0.23 ± 0.07	0.13 ± 0.03	0.10 ± 0.01	0.07 ± 0.00	0.01 ± 0.00
Brain	0.02 ± 0.01	0.01 ± 0.0	0.02 ± 0.01	0.01 ± 0.00	0.01 ± 0.00
Heart	0.12 ± 0.03	0.07 ± 0.01	0.06 ± 0.03	0.04 ± 0.01	0.02 ± 0.00
Lung	0.34 ± 0.02	0.20 ± 0.02	0.18 ± 0.02	0.12 ± 0.03	0.05 ± 0.01
Liver	0.20 ± 0.03	0.22 ± 0.02	0.21 ± 0.07	0.14 ± 0.01	0.07 ± 0.01
Spleen	0.15 ± 0.03	0.12 ± 0.02	0.11 ± 0.02	0.10 ± 0.01	0.06 ± 0.01
Stomach	0.08 ± 0.08	0.21 ± 0.05	0.17 ± 0.05	0.06 ± 0.03	0.03 ± 0.02
Kidneys	3.39 ± 0.58	3.01 ± 0.73	2.93 ± 1.20	2.73 ± 0.18	1.35 ± 0.23
Muscle	0.05 ± 0.01	0.03 ± 0.00	0.05 ± 0.01	0.02 ± 0.00	0.02 ± 0.00
Pancreas	0.08 ± 0.02	0.05 ± 0.01	0.02 ± 0.00	0.02 ± 0.00	0.01 ± 0.01
Bone	0.05 ± 0.01	0.04 ± 0.01	0.06 ± 0.02	0.03 ± 0.02	0.01 ± 0.00
Percent injected dose (%ID)					
Urine	95.60 ± 1.06	96.10 ± 1.40	97.0 ± 1.02	96.46 ± 2.29	95.90 ± 1.05
Intestines	0.45 ± 0.10	1.3 ± 0.80		1.70 ± 0.91	1.20 ± 0.57
Uptake ratio of tumor/normal tissue					
Tumor/blood	2.17	3.0		2.14	9.0
Tumor/muscle	10.0	13.0		7.5	4.5

Data are presented as %ID/g ± SD except for urine and intestines, values for which are expressed as %ID ± SD.

*P ≤ 0.02, significance comparison between radiolabeled peptide uptake without and with cold peptide at 2 h post injection.